

Los Alamos National Laboratory is operated by the University of California for the United States Department of Energy under contract W-7405-ENG-36

LA-UR--92-3223

DE93 003696

TITLE RADIATION CALCULATIONS USING MATH/SIMP/CINDER90

AUTHOR(S) Laurie Waters

SUBMITTED TO

## DISCLAIMER

This report was prepared as an account of work sponsored by an agency of the United States Government. Neither the United States Government nor any agency thereof, nor any of their employees, makes any warranty, express or implied, or assumes any legal liability or responsibility for the accuracy, completeness, or usefulness of any information, apparatus, product, or process disclosed, or represents that its use would not infringe privately owned rights. Reference herein to any specific commercial product, process, or service by trade name, trademark, manufacturer, or otherwise does not necessarily constitute or imply its endorsement, recommendation, or favoring by the United States Government or any agency thereof. The views and opinions of authors expressed herein do not necessarily state or reflect those of the United States Government or any agency thereof.

By publishing this report, the publisher acknowledges that the U.S. Government retains a nonexclusive, royalty-free license to publish or reproduce the published form of this report, and to allow others to do so, for U.S. Government purposes.

This report was prepared by Los Alamos National Laboratory, and its contents are work performed under the auspices of the U.S. Department of Energy.

**Los Alamos** Los Alamos National Laboratory  
Los Alamos, New Mexico 87545

FORM 2-80  
GPO 282-900-000

DISTRIBUTION OF THIS DOCUMENT IS UNLIMITED

# **RADIATION CALCULATIONS USING LAHET/MCNP/CINDER90**

Laurie Waters

*Los Alamos National Laboratory, MS H803*

*Los Alamos, New Mexico 87545*

## **ABSTRACT**

The LAHET Code System is now being used to address a variety of topics in radiation calculations needed by high energy physics. Recent improvements to the code are described, and two example calculations are presented. The first illustrates the use of the code in simulating low energy neutron response for the lead scintillator sampling calorimeter of Brookhaven experiment 814. The second describes the neutron fluence and activation calculations done for the forward calorimeter in the proposed SSC GEM detector.

## **1. Introduction**

The need for simulations of various radiation environments in accelerator projects such as SSC and LHC is well known. The possible damage to sensitive detectors and electronics must be estimated, and adequate protection designed. The contribution to detector background noise within the calculated environment must be studied. Aids are also needed in the design of shielding for detectors halls and access tunnels, not only for normal operations, but for possible disaster scenarios. Increasingly there is a demand for advance estimates of possible radiation doses for those servicing equipment, and for activation information for detector and accelerator components. Very similar calculations are also essential for lower energy, but high intensity proposals such as the design of neutron targets for Accelerator Transmutation of Wastes, and Advanced Neutron Sources. The LAHET Code System (LCS) is now being applied to many of these tasks. Along with a description of the code, two examples are described in this paper.

## **2. The LAHET Code System**

An overall diagram of the LCS is shown in figure 1. Further details for the CINDER90 activation code interface are given in figure 2. The Los Alamos High Energy Transport (LAHET) code<sup>1</sup> is a monte carlo simulation package in which various options for the tracking of hadrons, photons and electrons may be chosen. Source particle descriptions are either designated by the user or read in from an external file. Hadrons with kinetic energies greater than 5 GeV are followed with the FLUKA<sup>2</sup> code; those below 2 GeV with the HETC Bertini model or the ISABEL code<sup>3</sup>. A linear transition is made between those limits, which may also be adjusted by the user. Standard LAHET options<sup>1</sup> such as the RAL evaporation fission model, Fermi breakup for nuclei with A less than 20, and a preequilibrium model may be

selected. All photons and electrons are followed with EGS4, which has now been implemented into the LAHET package. Primarily as an aid to analysis of scintillator response, the  $H(n,n)$  and  $^{12}C+n$  reactions have been extended to .1 MeV directly in the LAHET code<sup>4</sup>. An interface to the TRACE<sup>5</sup> code has also been added to provide a substitute for the standard Birks formalism of scintillator light output. The enhanced LAHET package is referred to as SUPERHET.

Neutrons with kinetic energies less than 20 MeV are written to a file for further processing with the coupled neutron-photon monte carlo code MCNP<sup>6</sup>. The current version, MCNP4, will fully track not only photons from the  $(n,\gamma)$  reactions, but electrons produced by the gammas as well. The MCNP surface based geometry package is used throughout the LCS.

Spallation products produced by SUPERHET and the neutron fluences from MCNP form the input into the CINDER90<sup>7</sup> activation code, where their subsequent decay is tracked over time. Currently CINDER90 supports a library of 736 targets and 12023 reactions.

### 3. The E814 Participant Calorimeter

One element of Brookhaven AGS Experiment E814 is a lead/scintillator sampling calorimeter known as the Participant Calorimeter (PCAL). Figure 3 shows the construction of this device<sup>8</sup>. The PCAL consists of four identical quadrants arranged around the beam (fig. 3a). Each quadrant is subdivided into four "pie" shaped slices of  $22.5^\circ$  each, and each pie is further divided radially into eight towers. Each tower is read out by a scintillator plate with the signal carried by a scintillating fiber coupled along the edge of the plate. Longitudinally, the calorimeter consists of alternating layers of the 0.3 cm thick scintillator and 1.0 cm lead absorber plates. The scintillator plates lie in 0.1 cm polypropylene trays. The PCAL is divided into 4 segments (fig. 3b); the first electromagnetic (EM1) consisting of 6 Pb/sci sections, the second electromagnetic (EM2) consisting of 6 Pb/sci sections, the first hadronic (HAD1) with 24 Pb/sci sections and the second hadronic (HAD2) with 23 Pb/sci sections. Each of the four segments is further separated by 1.6 cm steel plates for support. The PCAL contains a total of 4 hadronic interaction lengths.

Figures 4 through 6 show the results of the LCS simulations with 2.46 GeV/c momentum pions and protons, using data taken at the AGS<sup>9</sup>. Figure 4 shows the total energy contained in the PCAL for protons and pions. MCNP unfortunately does not track the charged particle products of low energy neutron interactions; therefore these particles must be regenerated by using the MCNP neutron fluence as a source input into SUPERHET. The effect of the low energy neutrons is illustrated by comparing the simulation results with SUPERHET alone, and with the MCNP/SUPERHET analysis added in. The effect of adding in the response of neutrons with kinetic energies less than 20 MeV is to increase the energy deposition upward by about 10%.

Energy deposition is shown within the various segments for the pions in figure 5. The tails of the distributions are well reproduced, and no renormalization at all

is required to match the data. The proton radial distribution is shown in figure 6. In the simulation, the energy per unit area deposited in concentric rings of 4 cm width centered around the beam axis is shown. The points are joined with a solid line to guide the eye. Again, the simulations are in good agreement with the data.

#### 4. The GEM Forward Calorimeter

The simulation of the GEM FCAL used in this illustration is shown in figure 7. The device was divided into 16 segments for the calculation, of which segment 1 is the most active. The FCAL is composed of 92.9% by volume tungsten absorber (WN507C), 6.4% liquid Argon, and .7% kapton/copper readout elements. Shown in figure 8 are the distribution of spallation products from SUPERHET and the neutron fluence from MCNP which form the input into CINDER90. Structures in the neutron fluence due to resonances in the neutron scattering and absorption spectra, notably the dip at 10 eV, are easily recognized. The fluence, when plotted as  $dN/d(\ln E)$  is essentially a gaussian peaked around .1 MeV. In similar calculations for other materials, it is quite notable that the positioning of the peak is largely determined by the size of the detector and the magnitude of the neutron elastic scattering cross section. The shape of the peak is determined by the overlap with elastic and absorption resonances. Such resonances are positioned far below the peak of the FCAL data and do not disturb its shape.

Figure 9 summarizes the activity density for the FCAL section 1 over 30 time steps. The primary beam is assumed to run for 6 months, then shut off. The subsequent decay is followed for another 6 months. The sudden fall off at shutdown is due to the disappearance of various short lived excited nuclear states. At shutdown, a maximum activity density of  $1.1 \times 10^{-4}$  ci/cc is reached (3.3 ci integrated over Section 1). The plot also illustrates the contribution of the low energy neutron interactions to the calculation. The lowest curve on the plot represents the calculation only for SUPERHET spallation products. Other curves show the increase in activity as the neutron fluence for various energy ranges is added in. Note that one day after shutdown, the original spallation products account for 20% of the activity. One major long lived nuclide accounting for much of the activity is  $W^{185}$ , contributing 30% after 6 months of beam, and 63% one day later.

Much other data is available from the calculation. Figure 10 shows the decay power, i.e., total energy of the decay gammas and electrons, in Watts/cc. Not all of the gamma spectra for decaying nuclides are available in the standard libraries. To make up the difference, each unknown nuclide was assigned a spectrum from the known data based on the even-ness or oddness of its Z and A, and from the Q value of the reaction. The unknowns are quite short lived, as is illustrated in the figure 10.

To obtain the equivalent dose from the region several approaches are possible. One which illustrates the self-shielding properties of the material is illustrated in figure 11. A Point kernel shielding calculation was made with the major radionuclide sources in Section 1 after 1 day of cooling. The detector was modelled as an

infinite slab of material with varying thickness, and the equivalent dose calculated at the front of the slab. Little contribution is seen from gamma sources deeper than 2 cm.

## 5. Conclusions

The LCS and CINDER code systems continue to be used to calculate needed parameters for many types of accelerator based operations. Current work includes the evaluation of neutron fluences at GEM and SDC, as well as activation of forward elements in both detectors. Details of detector response to low energy neutron and photon backgrounds are also being studied. The code is also highly important to the design of neutron source at a variety of facilities.

## 5. Acknowledgements

The contributions of the LCS and CINDER90 code developers and applications experts are gratefully acknowledged, especially Avigdor Gavron, Richard Prael, Bill Wilson, Tal Englund, Grady Hughes and Henry Lichtenstein. I would also like to thank our collaborators at LAMPF and SSC, especially David Lee, Andrea Palounek and Michael Marx.

## 6. References

1. R. E. Prael and H. Lichtenstein, "User Guide to LCS: The LAHET Code System", Los Alamos National Laboratory (Sept 15, 1989).
2. P. A. Aarnio, et. al, "FLUKA89" (issued by CERN).
3. Radiation Shielding Information Center, "HETC Monte-Carlo High-Energy Nucleon-Meson Transport code", Report CCC-178, Oak Ridge National Laboratory (1977).
4. A. Gavron, *Nucl. Instr. & Meth.* **A313** (1992) 161.
5. W. C. Sailor, R. C. Byrd and Y. Yariv, "TRACE: A Monte Carlo Code for the Efficiency of Multi-Element Neutron Scintillator Detectors", Los Alamos report LA-11348-MS (1988), unpublished.
6. J. F. Breisemeister, ed., "MCNP - A General Monte Carlo Code for Neutron and Photon Transport", LA 7396-M Rev. 2, Los Alamos National Laboratory (1986).
7. D. M. Lee, W. W. Kinnison and W. B. Wilson, "A Monte Carlo Calculation of the Neutron Flux in the L<sub>2</sub> Detector", presented to the IEEE Nuclear Science Symposium, December 1990, LANL preprint LA-UR 90 2954
8. J. Simon Gillo, et. al, "The Design and Construction of a Pb/Scintillator Sampling Calorimeter with Wavelength Shifter Fiber Optic Readout", submitted to *Nucl. Instr. & Meth.*
9. D. Fox, et. al, "Response of the Participant Calorimeter to 4.5-6.8 GeV/c

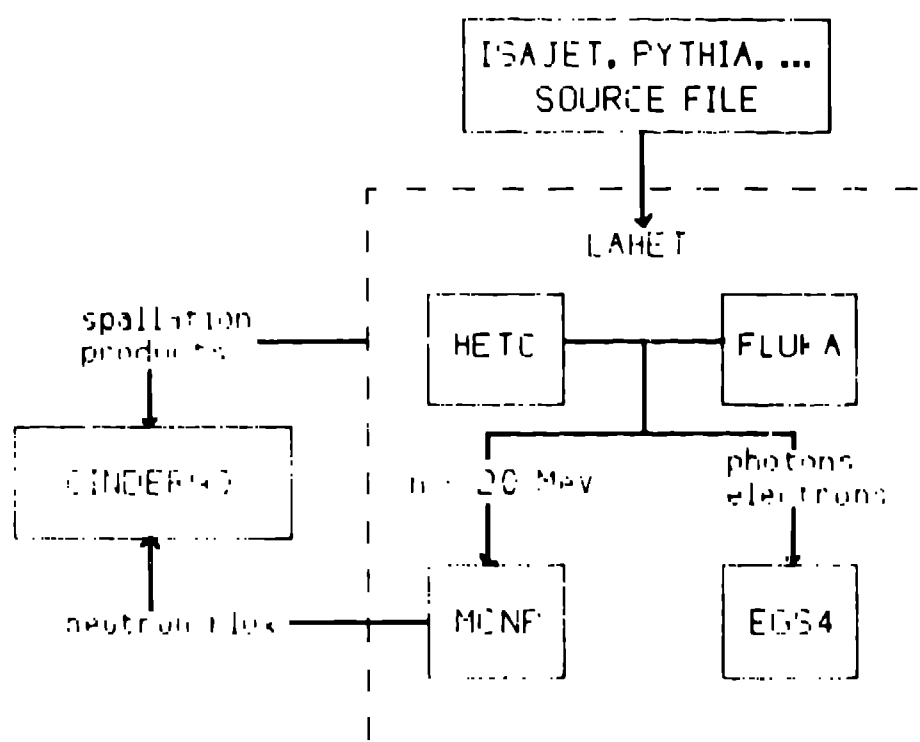


Fig. 1 Overview of the ICS system

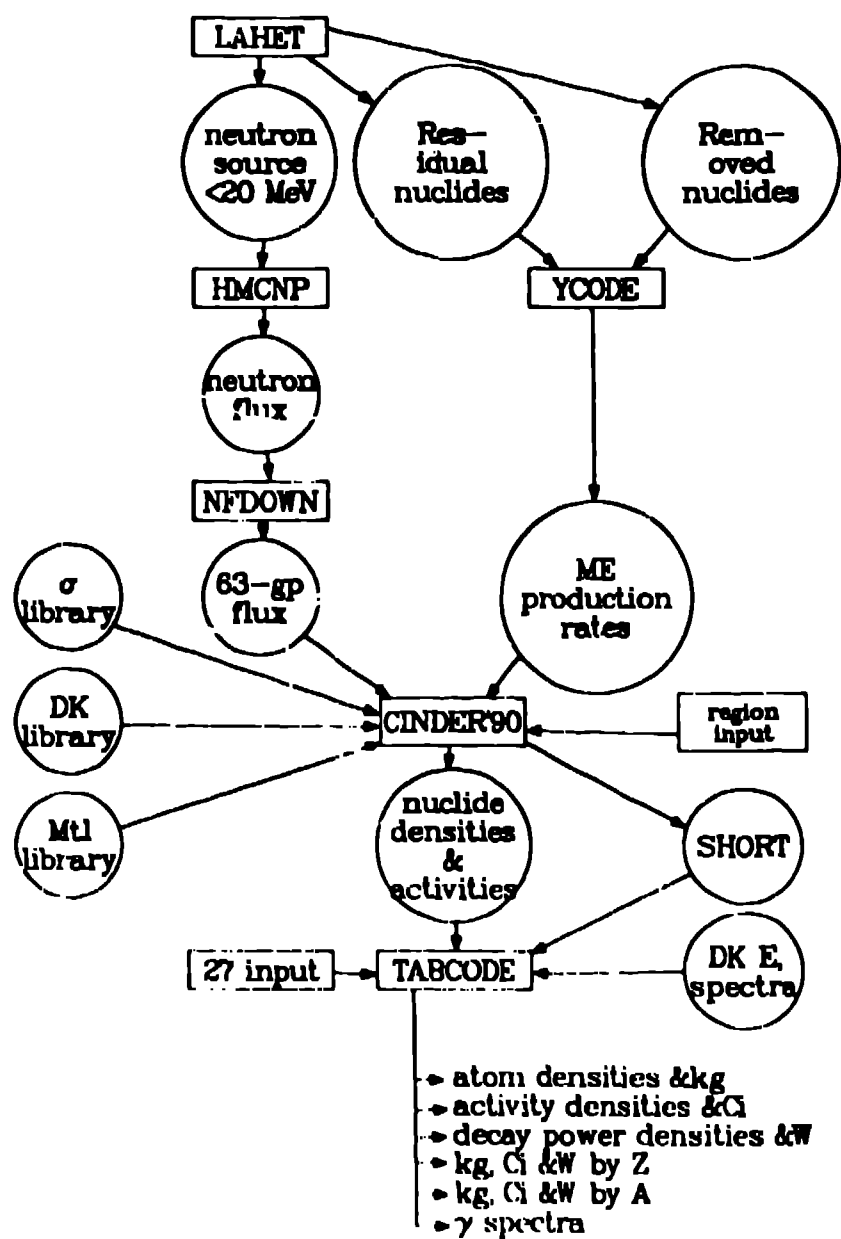


FIG. 2 Overview of the CINDER90 system

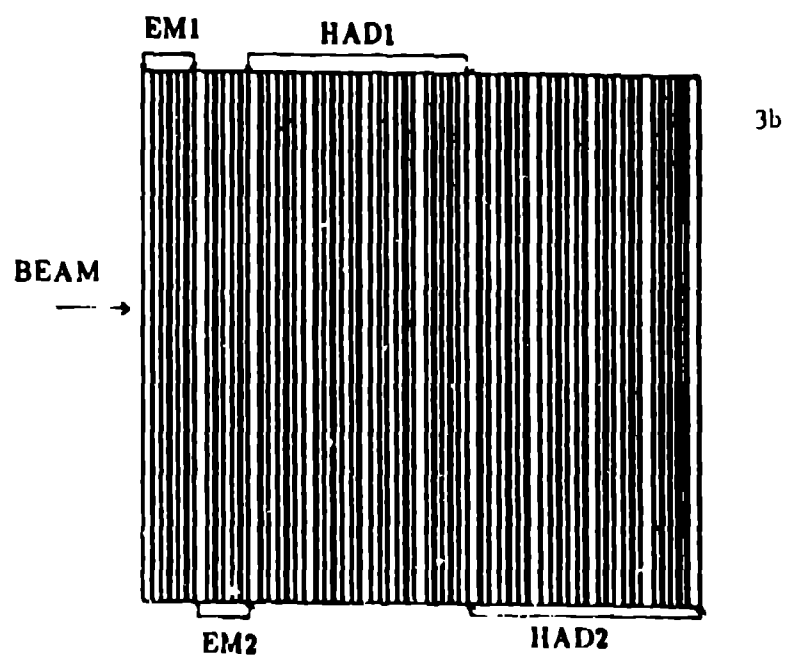
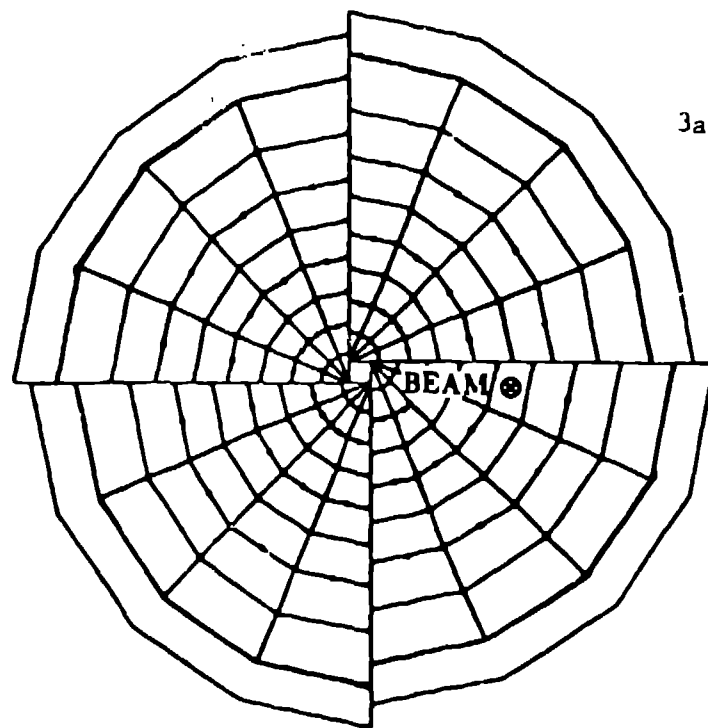


Figure 3.  
E814 Participant Calorimeter  
a) downstream view  
b) longitudinal view



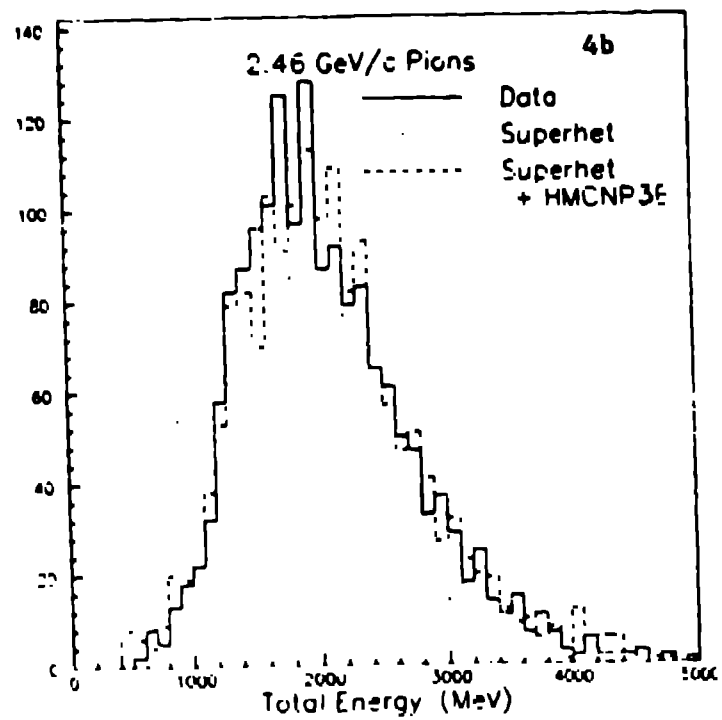
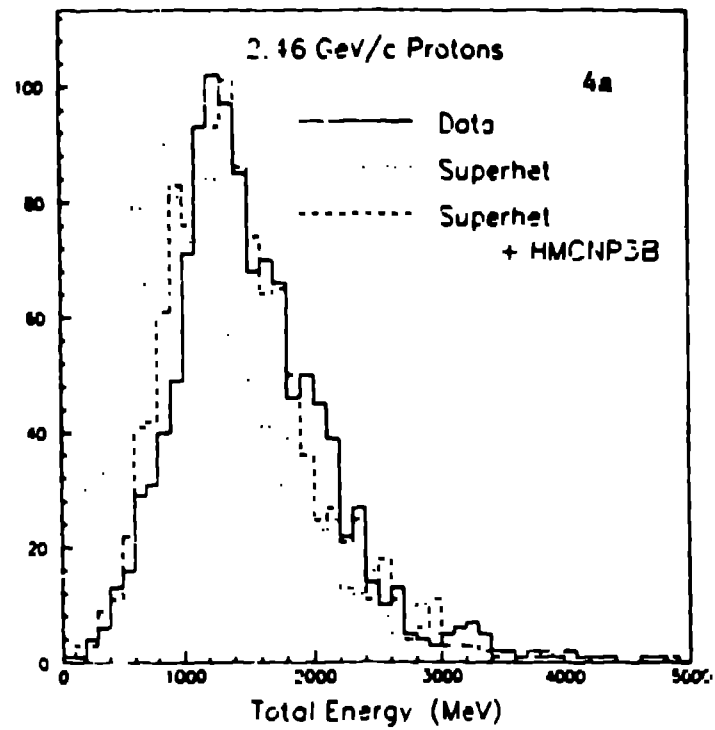


FIGURE 4: Effect of low energy neutrons

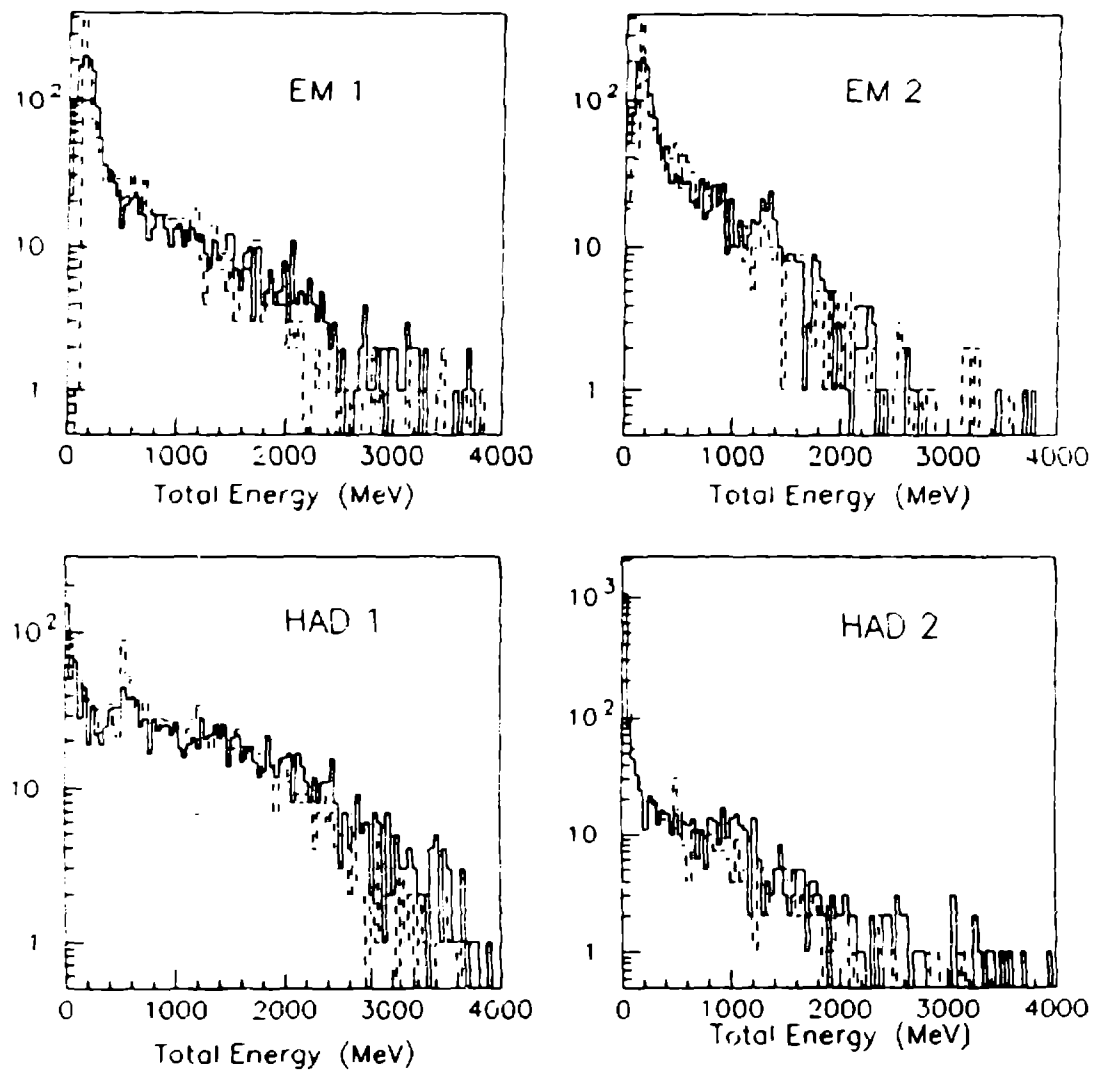


FIGURE 5 : 2.46 GeV/c pions, energy deposited in various segments (data - solid) (simulation - dashed)

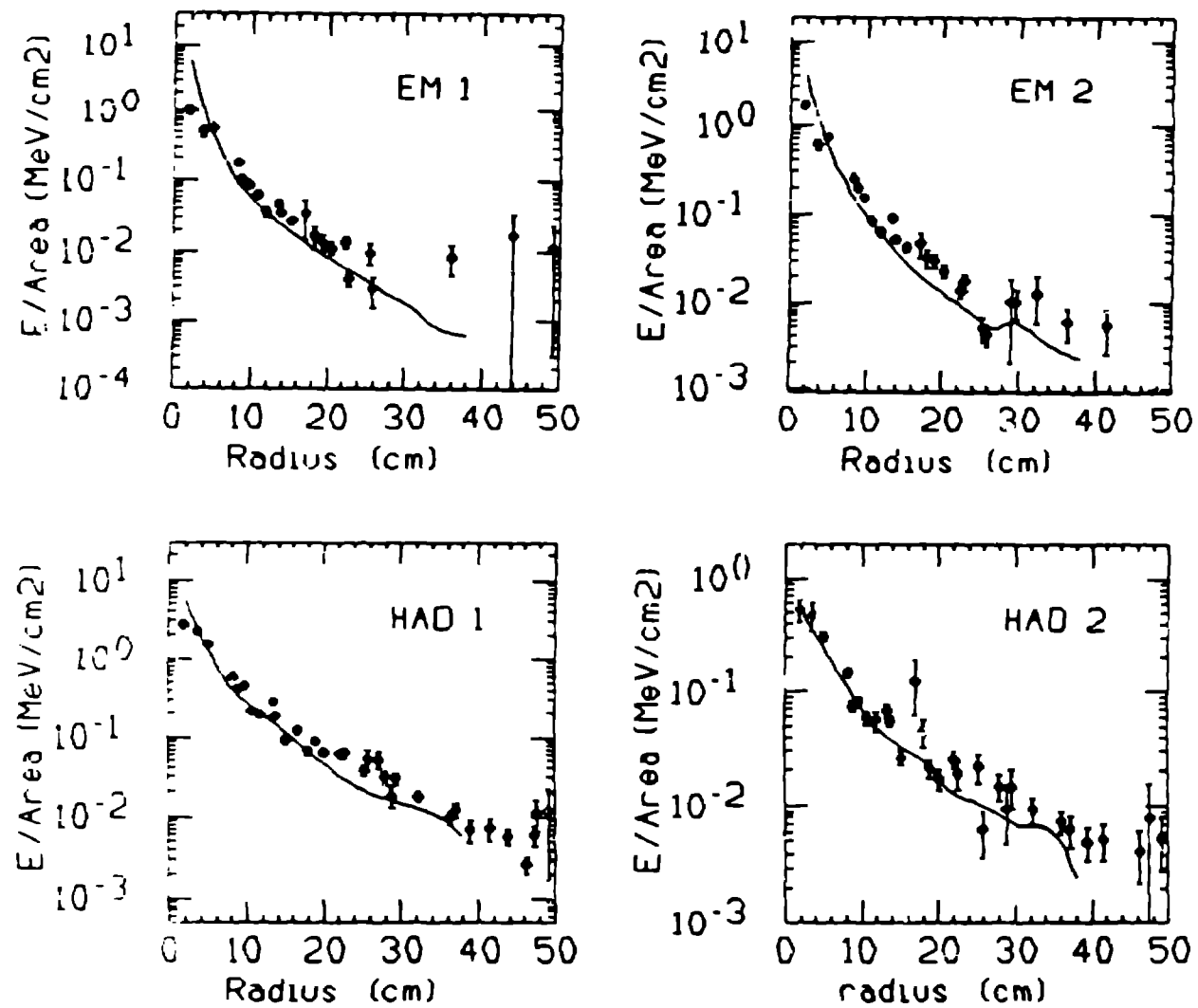


FIGURE 6: 2.46 GeV/c protons , radial energy distribution

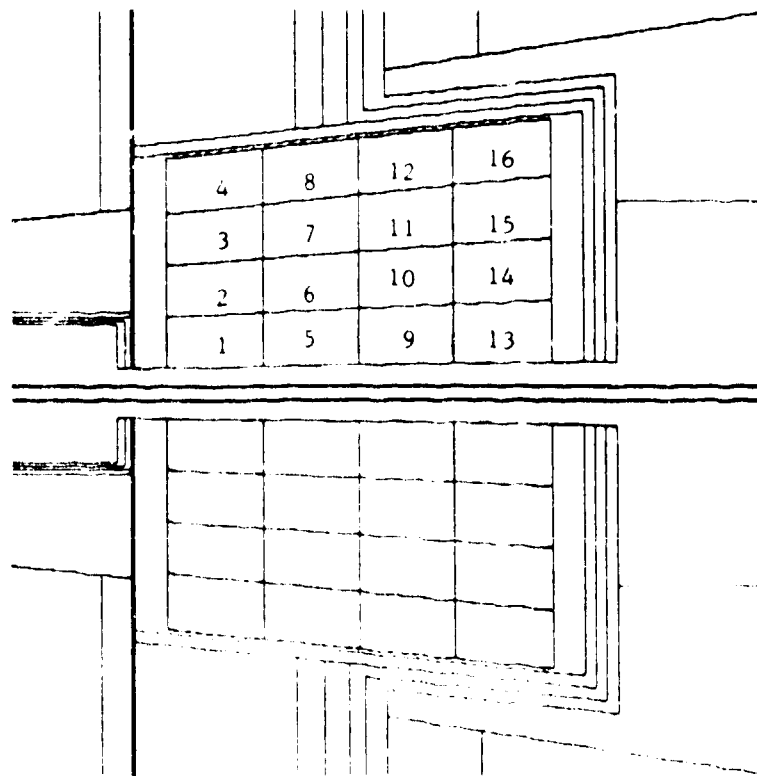
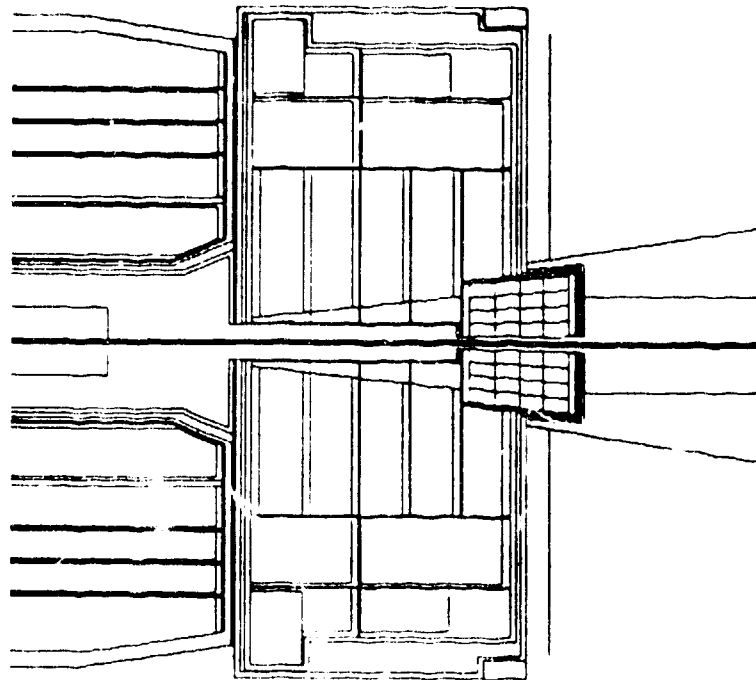


FIG. 7 The GEM Forward Calorimeter

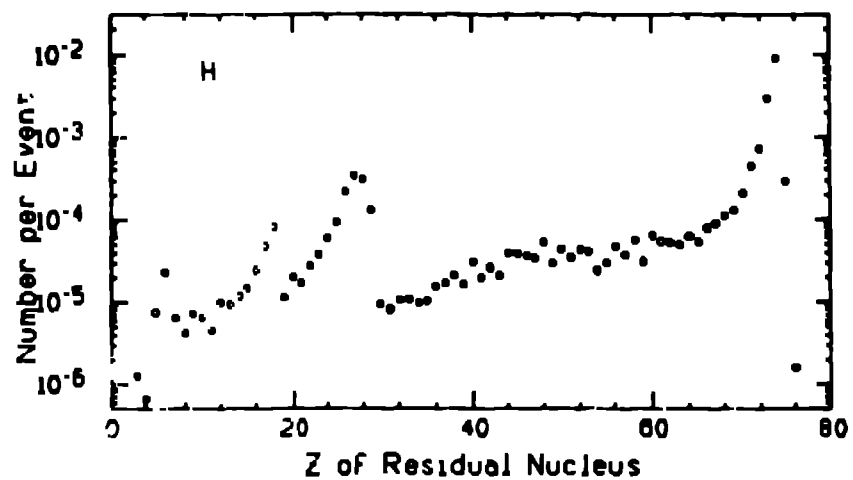


Fig. 8a Distribution of Spallation Products in Z

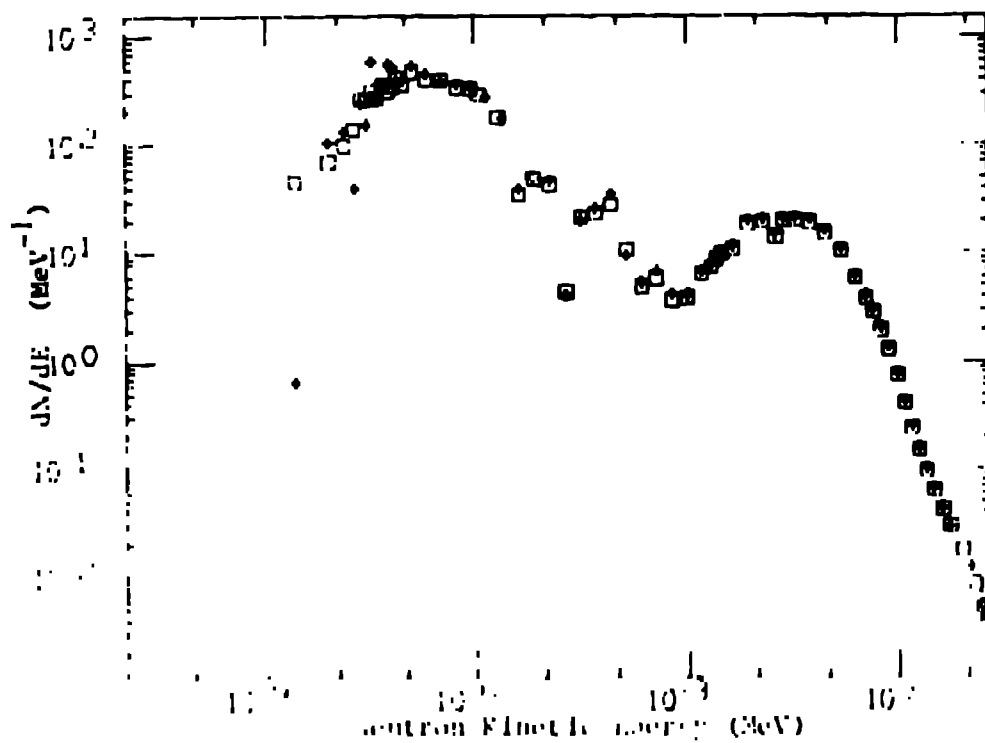


Fig. 8b Neutron Fluence in Section 1. The two sets of points represent a doubling of statistics by running 250 and 500 DETDET primary events.

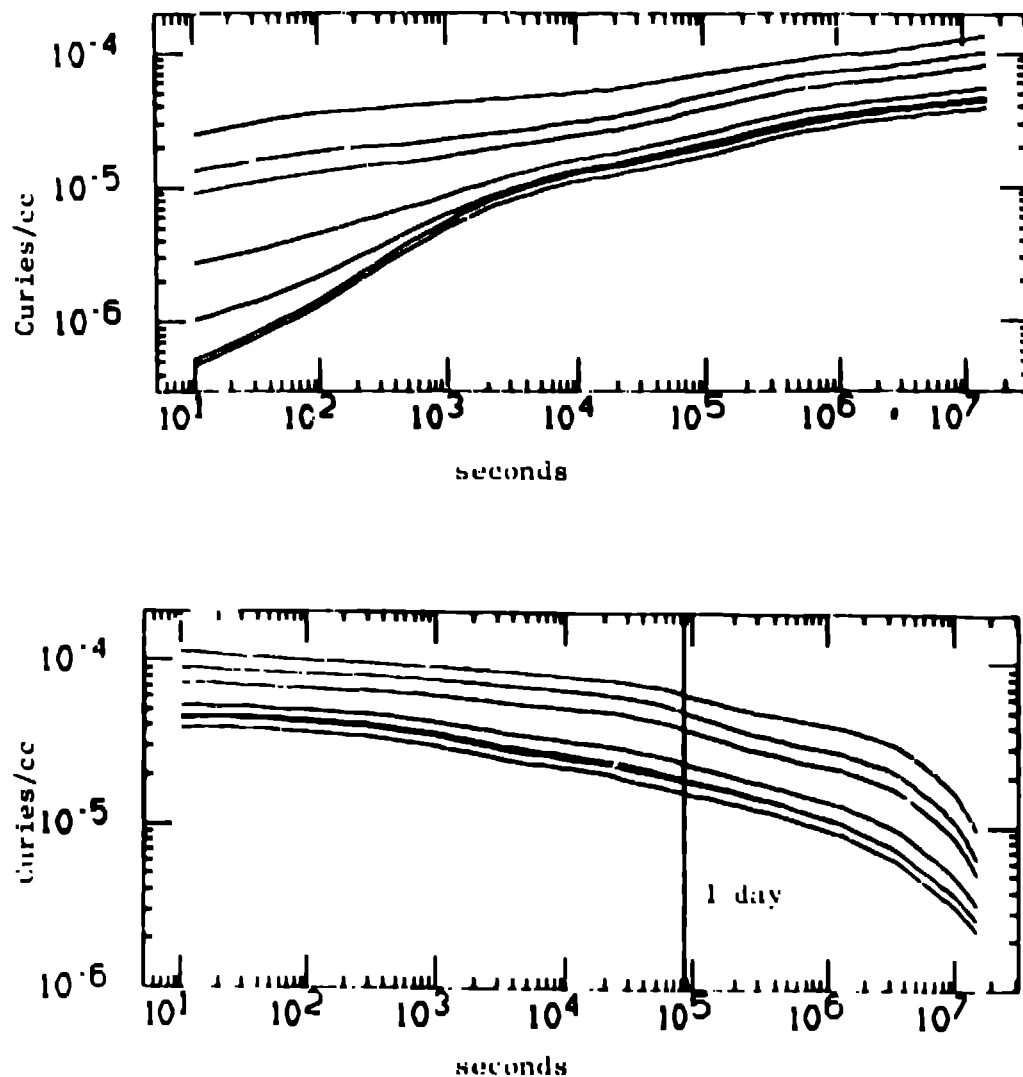


Fig. 9 Activity density for Section 1. The top figure is the calculation with beam on for 6 months. The decay is followed for another 6 months after shutdown (bottom). From top to bottom, the curves represent:

- full calculation
- spallation  $\phi$  neutrons with  $E$  less than 1 MeV
- spallation  $\phi$  neutrons with  $E$  less than 100 keV
- spallation  $\phi$  neutrons with  $E$  less than 10 keV
- spallation  $\phi$  neutrons with  $E$  less than 100 eV
- spallation alone.

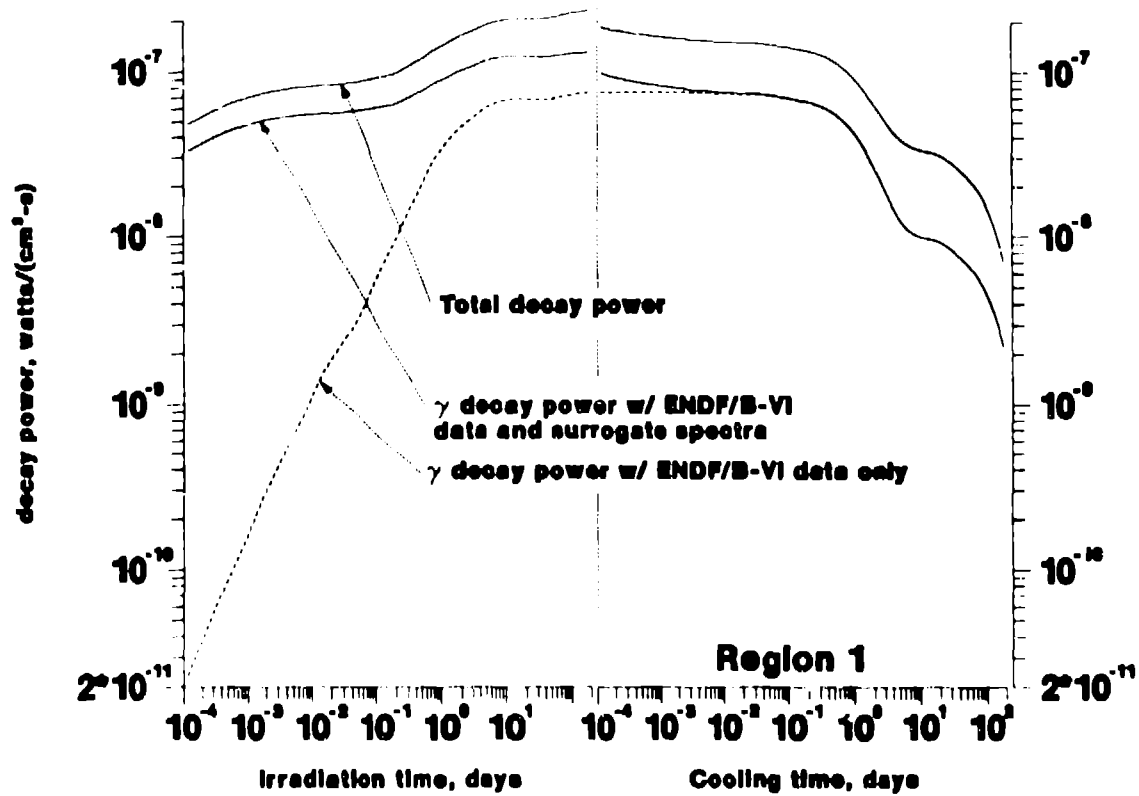


Fig. 10 Comparison of  $\gamma$  decay power calculated with CINDER90 using processed ENDF/B-VI spectral data with and without surrogate data for nuclides not included in ENDF/B-VI.

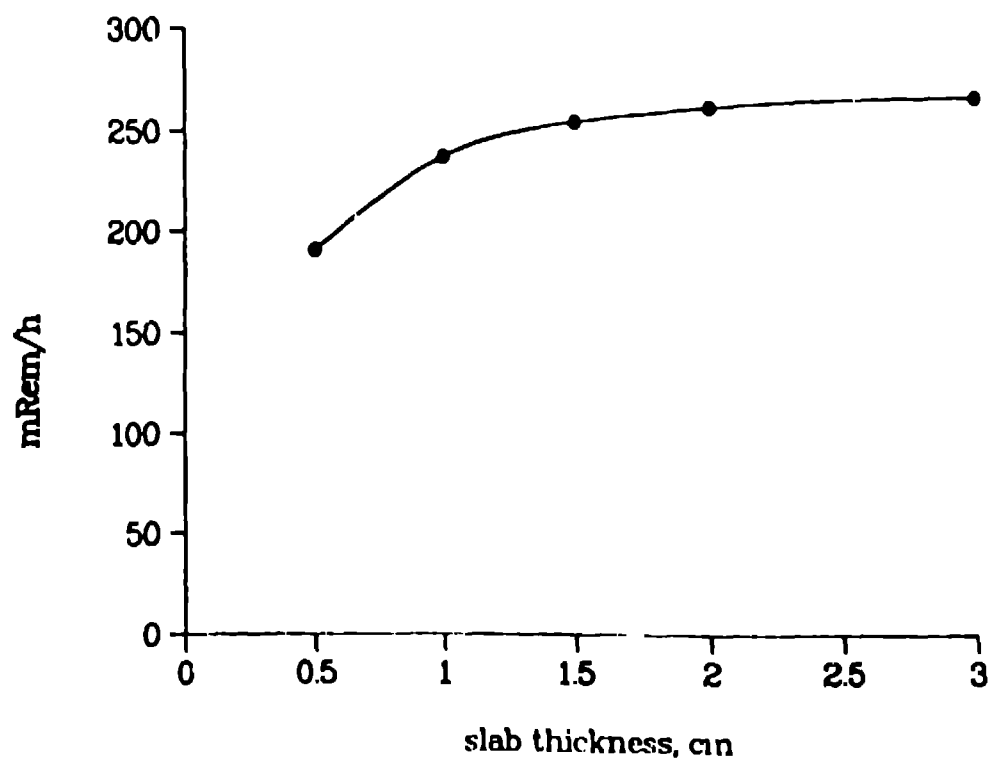


FIG. 11 Dose-equivalent rate (mRem/h) 10 cm from slab face for region 1 inventory at 1 day cooling.